

In-plane optical conductivity of $\text{La}_{2-x}\text{Sr}_x\text{CuO}_4$: Reduced superconducting condensate and residual Drude-like response

S. Tajima^{1)*} and Y. Fudamoto^{1)*}, T. Kakeshita^{1,2)}, B. Gorshunov^{3)**},
V. Železný^{1)***}, K. M. Kojima²⁾, M. Dressel³⁾, and S. Uchida²⁾

¹⁾Superconductivity Research Laboratory, ISTEK, 1-10-13 Shinonome, Tokyo 135-0062, Japan

²⁾Dept. of Physics, The University of Tokyo, Tokyo 113-8656, Japan

³⁾I. Physikalisches Institut, Universität Stuttgart, D-70550 Stuttgart, Germany

(Dated: February 2, 2008)

Temperature dependences of the optical spectra of $\text{La}_{2-x}\text{Sr}_x\text{CuO}_4$ with $x=0.12$ and 0.15 were carefully examined for a polarization parallel to the CuO_2 -plane over a wide frequency range down to 8 cm^{-1} . Selection of well-characterized crystals enabled us to measure purely in-plane polarized spectra without any additional peak. The weight of superconducting (SC) condensate estimated from the missing area in $\sigma_1(\omega)$ well agrees with the estimate from the slope of $\sigma_2(\omega)$ vs $1/\omega$ plot, showing no evidence that the Ferrell-Glover-Tinkham sum-rule is violated in the optical spectrum. We demonstrate that the optically estimated SC condensate is much smaller than the value obtained from the μSR measurement of magnetic penetration depth. We also find an anomalous increase of conductivity in sub-millimeter region towards $\omega=0$ below T_c , which suggests the microscopic inhomogeneity in the superconducting state. Both observations are discussed in relation with the inhomogeneous electronic state that might be inherent to high- T_c cuprates.

I. INTRODUCTION

The superconducting (SC) condensate, one of the essential parameters for a superconductor, has been a subject of discussion in high- T_c superconducting cuprates (HTSC). The recent progress in scanning tunneling spectroscopy has revealed a strange inhomogeneous distribution of the gap in $\text{Bi}_2\text{Sr}_2\text{CaCu}_2\text{O}_8$ (BSCCO)¹. The effect of this real-space gap inhomogeneity on a superconducting (SC) condensate is unclear. On the other hand, the angle-resolved photoemission spectroscopy (ARPES) has demonstrated a distinct k -dependence of the gap at the Fermi surface in the pseudo-gap state or the stripe ordered state^{2,3}. For the system with such a partially gapped Fermi surface, the source of SC condensate is not obvious.

As one of the direct methods to detect a SC gap and the weight of SC condensate, optical studies have been extensively performed for HTSC. A clear conductivity depression was observed below $\sim 500\text{ cm}^{-1}$ in $\text{YBa}_2\text{Cu}_3\text{O}_y$ (YBCO)^{4,5,6,7} and BSCCO⁸. Then, the weight of SC condensate ($\rho_s \sim \omega_{ps}^2$) was estimated from the missing area (A) of the real part $\sigma_1(\omega)$ of conductivity spectrum or from the low-frequency behavior of its imaginary part $\sigma_2(\omega)$.

The estimate of SC condensate from optical spectra, however, has been subject to uncertainty. One of the reasons is that, unlike the case of conventional superconductors, there often remains some conductivity below the gap energy, forming a Drude-like increase towards $\omega=0$ ⁹. Since the missing area of $\sigma_1(\omega)$ is large in YBCO and BSCCO, the remaining conductivity effect is relatively small in estimation of SC condensate. By contrast, in the case of lower T_c -HTSC such as $\text{La}_{2-x}\text{Sr}_x\text{CuO}_4$ (LSCO), it must give more serious effect. Nevertheless, this residual conductivity was ignored in most of the previous estimate of SC condensate except for a few works^{10,11}. The origin

of this remaining conductivity is an important problem to be solved.

The other reason for the difficulty in determining SC condensate of LSCO is linked to the difficulty in obtaining a pure in-plane spectrum. Since the early stage of HTSC research, various different in-plane spectra have been reported for LSCO^{10,11,12,13,14} and $\text{La}_2\text{CuO}_{4+\delta}$ ¹⁵. Some of the reported in-plane spectra show rich features in a far-infrared (FIR) region^{13,14,15}, which are ascribed either to the LO-phonons¹³ or to the excitation related to the polarons¹⁴. According to the variety of spectra, different values of the SC condensate were derived, ranging from 250 to 430 nm ^{10,11,12,13,14,15} in terms of the London penetration depth $\lambda_L^{\text{FIR}} (=1/2\pi\omega_{ps})$, which do not correlate with the T_c -value of the studied sample. Some of them are considerably different from the value determined by μSR measurements^{16,17}.

The purpose of this work is two-fold. The first one is to clarify the origin of such a confusing situation in optical study of LSCO. We report a purely in-plane polarized spectrum of LSCO and demonstrate the effect of the c -axis component mixing, by comparing with the "dirty" spectra contaminated by the c -axis component. Possible reasons for the c -axis component mixing are discussed. The second and main purpose is to examine the electrodynamic response in the low energy region and to estimate the SC condensate, based on the purely in-plane polarized optical spectra of $\text{La}_{2-x}\text{Sr}_x\text{CuO}_4$ ($x=0.12$ and 0.15). The spectra were measured over a wide range of frequency $8 - 30000\text{ cm}^{-1}$, down to the sub-millimeter region. At $T \ll T_c$, we have found a depression of conductivity below 200 cm^{-1} (70 cm^{-1}) for $x=0.15$ ($x=0.12$) but a steep increase of the conductivity below 40 cm^{-1} (10 cm^{-1}), which leads to a significantly small missing area compared to the value estimated from the London length λ_L determined by μSR measurement. We conclude that a discrepancy of the SC condensate between the opti-

cal and μ SR-estimations is commonly observed in many HTSC. Possible scenarios for these anomalous features are discussed.

II. EXPERIMENTS

Single crystals of $\text{La}_{2-x}\text{Sr}_x\text{CuO}_4$ with $x=0.12$ and 0.15 were grown by a traveling solvent-floating zone (TSFZ) method. The superconducting transition temperature T_c is 36K for $x=0.15$ and 30K for $x=0.12$. Fixing crystal axes by observing X-ray Laue patterns at the surface of as-grown crystal rods, we cut the crystals along the c -axis and took several pieces of samples with a thickness of about 2 mm. We call them " ac -face" sample hereafter. For comparison, we also cut some crystal pieces with the c -axis perpendicular to the measurement surfaces called " ab -face" sample. In both cases, a - and b -axes are not distinguished although there is a small difference between them. After a number of trial measurements of far-infrared spectra, we realized that even Laue-characterized crystals were sometimes multi-domains, showing the c -axis phonon admixture.

The second characterization method to detect multi-domain is to observe the surface using a polarized optical microscope. Prior to this observation, the sample surfaces were polished with Al_2O_3 powder of different particle sizes at several steps. The particle diameter for the final polishing was $0.3\text{ }\mu\text{m}$. It was found that some pieces of crystals consisted of multi-domains. We carefully selected the single domain crystals for measurement of purely in-plane polarized spectrum. A typical diameter of the sample disks is about 5 mm. A spot size of the incident light is about 3 mm, well smaller than the sample size.

Optical reflectivity spectra were measured using a coherent-source spectrometer¹⁸ in a millimeter and sub-millimeter wavelength region ($8 - 33\text{ cm}^{-1}$), a Fourier transformation type spectrometer for infrared region ($30 - 8000\text{ cm}^{-1}$) and a grating type one for higher energy region above near-infrared ($4000 - 30000\text{ cm}^{-1}$). Both a sample and a gold mirror were mounted on a copper plate in a He-gas flow cryostat for temperature control. Before each measurement of a sample spectrum, a spectrum of gold mirror was measured as a reference. Reflectance of polarized light was measured with the s-polarized geometry at the incident angle of about 5 degree.

In order to compare the SC condensate estimated from the other experimental methods, we measured the London penetration depth using muon spin rotation (μ SR) technique. To improve the reliability of the missing area analysis and discussion, the μ SR measurement has been carried out on the same single crystal as used in the optical study. The analysis of the field distribution of a vortex lattice in the applied transverse field $H_t=0.2\text{ Tesla}$ has been performed using a London model¹⁹ with a Lorentzian cut-off²⁰ of 4.5-6.5 nm as a non-local correction. Other possible contributions for the broaden-

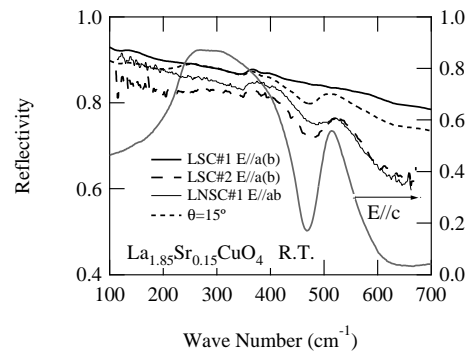


FIG. 1: Comparison of the in-plane reflectivity spectra of three $\text{La}(\text{Nd})_{1.85}\text{Sr}_{0.15}\text{CuO}_4$ crystals at 300K. LSC#1 and LSC#2 were measured on the ac -faces, while LNSC#1 is the spectrum for the ab -face measured without polarizer. The spectra of LSC#2 and LNSC#1 show a substantial contribution from the c -axis spectrum. The c -axis spectrum of LSCO is indicated by a dashed curve as a reference. We can reproduce a similar profile to LSC#2 and LNSC#1, using the pure in-plane spectrum (LSC#1) and the c -axis spectrum, as described in the text. The calculated reflectivity assuming a 15 degree rotation around the ac -/ bc -plane or equivalently the 6.7%-admixture of the c -axis component is indicated by a dash-and-dot curve.

ing of the field distribution, such as random pinning, are corrected by assuming an additional Gaussian relaxation with the relaxation rate 0.39-0.43 MHz.

III. RESULTS AND ANALYSIS

A. Effect of c -axis component admixture

Figure 1 shows the far-infrared reflectivity spectra at room temperature for several samples. LSC#1 is the almost perfectly in-plane polarized spectrum for the ac -face of $\text{La}_{1.85}\text{Sr}_{0.15}\text{CuO}_4$ crystal, while LSC#2, the spectrum for another ac -face $\text{La}_{1.85}\text{Sr}_{0.15}\text{CuO}_4$ crystal, shows the bumps centered at around 300 cm^{-1} and 520 cm^{-1} . LNSC#1, measured without polarizer for the ab -face of $\text{La}_{1.45}\text{Nd}_{0.4}\text{Sr}_{0.15}\text{CuO}_4$, also shows a similar bump-like feature at the same position. Compared to the c -polarized spectrum ($E \parallel c$) in Fig.1, these bumps can be assigned to the two A_{2u} mode phonons with the TO-frequencies of 240 cm^{-1} and 500 cm^{-1} that are the c -axis vibration modes of oxygens²¹. Namely, the bumps result from mixing of the c -polarized component into the in-plane spectrum.

We can reproduce a similar spectrum to LSC#2 and LNSC#1, using LSC#1 as a pure in-plane reflectivity data ($R_{a/b}$) and the measured c -polarized reflectivity data (R_c), with $R_\theta = R_{a/b}\cos^2(\theta) + R_c\sin^2(\theta)$. The dashed curve in Fig.1(a) represents the calculated reflectivity spectrum for $\theta=15$ degree deviation of the polarization direction from the pure $a(b)$ -axis or equivalently the

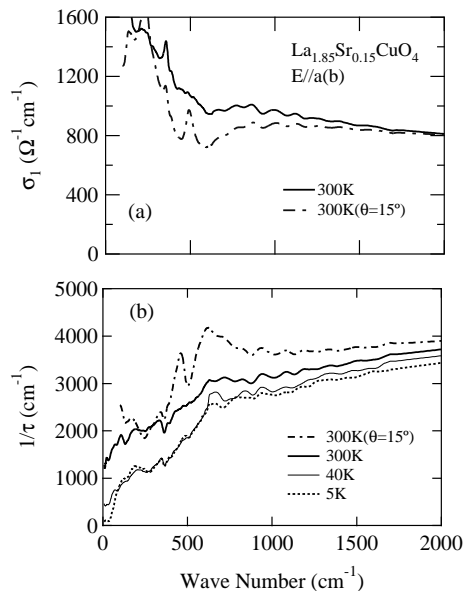


FIG. 2: (a) Comparison of the in-plane conductivity $\sigma_1(\omega)$ of $\text{La}_{1.85}\text{Sr}_{0.15}\text{CuO}_4$ (LSC#1) and the c -axis component mixed data for $\theta=15$ degree. (b) Comparison of the scattering rate $1/\tau(\omega)$ for LSC#1 and the c -axis component admixture case. It is clear that the double peak is a result of the c -component admixture. It is also demonstrated that the kink at $\sim 700 \text{ cm}^{-1}$ even at 300K and is independent of the superconducting response below 200 cm^{-1} .

6.7%-admixture of mis-oriented volume. Corresponding to the rapid drop of reflectivity above 600 cm^{-1} , the dip at $\omega \sim 470 \text{ cm}^{-1}$ and the suppression below 250 cm^{-1} in the c -axis spectrum, the weak reflectivity suppressions giving the bump features in LSC#2 and LNSC#1 are well reproduced in the calculated spectrum.

The admixture of the c -axis spectral component into the in-plane spectrum seriously influences the conductivity and scattering rate spectra calculated from the reflectivity spectrum via Kramers-Kronig (KK) transformation. As shown in Fig.2(a), the c -component admixture creates the conductivity dip between 300 and 1000 cm^{-1} and the peak around 500 cm^{-1} . These additional features were observed in both of conductivity and reflectivity spectra for the previous studies of LSCO^{13,14} and $\text{La}_2\text{CuO}_{4+\delta}$ ¹⁵, which clearly indicates the admixture of the c -axis component. Figure 2(b) demonstrates that the double peak in $1/\tau(\omega)$ reported by Startseva *et al.*¹³ can also be considered as the same admixture effect.

There are several possible reasons for the c -axis component mixing, such as (i) mis-cut of crystals, (ii) multi-domains in as-grown crystals, (iii) p -polarization admixture in non-polarized measurement. Mis-cut of as-grown crystal is the most primitive mistake that gives a mis-oriented surface for reflectivity measurement. This problem is peculiar to the LSCO crystals, because the cutting procedure is inevitable for extracting an appropriate size sample from an as-grown crystal rod. In the case of

YBCO crystals grown by a flux method, natural surfaces can be used for optical measurement, and the BSCCO crystals grown by a TSFZ method are so easily cleaved that crystal cutting is not necessary to extract the ab -face samples.

The multi-domain problem is serious in the TSFZ crystals. It often appears in the early stage of crystal growth, namely, in the crystal portion close to a seed. It is hard to confirm that a sample is of single domain by a usual X-ray Laue pattern measurement, because a typical X-ray spot size is much smaller than the sample surface area of about $3 \times 3 \text{ mm}^2$. This was the case for LSC#2. In order to scan the whole area of sample surface, we need an X-ray topography measurement. An easier way to examine the existence of multi-domain feature is to observe a polished sample surface using a polarized optical microscope. In the worst case, even the sample selected by this method shows some admixture of different direction component in its far-infrared spectrum. The mis-oriented domain behind the surface within a penetration depth ($\sim 1 \mu\text{m}$) of far-infrared light is a possible origin. The dielectric response of the light penetrating through multi-domains must be complicated, giving an unusual structure in far-infrared spectra. The obtained reflectivity cannot merely be interpreted as a weighted summation of the in-plane component $R_{a/b}$ and the c -axis component R_c in this case.

The final problem related to the p -polarization must be considered when we measure the in-plane spectrum on the ab -face using non-polarized light. In order to gain a signal, we sometimes did not use a polarizer for the ab -face measurement because the light intensity is reduced to about a half when going through a polarizer. However, this geometry measurement always gave a weak bump-like feature that roughly corresponds to the c -axis phonon peak or high-frequency reflectivity suppression. An example is shown in Fig.1(a) as LNSC#1 for the ab -face of $(\text{La},\text{Nd},\text{Sr})_2\text{CuO}_4$ crystal which was well characterized by an X-ray diffraction. A similar problem can be seen in the set of data by Lucarelli *et al.*¹⁴ About a half of the seven spectra were measured on the ab -face without a polarizer, and they show a clear peak corresponding to the c -axis phonon²². The most plausible origin of this c -axis component mixing is the p -polarization component in the non-polarized light, as van der Marel *et al.* pointed out²³. Although the introduced c -component is very small if the surface is perfectly ab -oriented, the effect possibly becomes evident in extremely anisotropic materials like HTSC.

All the problems due to the c -axis component mixing become serious only in strongly anisotropic systems, namely, when the reflectivity values are remarkably different in the ab - and c -polarized spectra. This is well demonstrated in the optical spectra of intentionally mis-aligned films of $(\text{La},\text{Ce})_2\text{CuO}_4$ ²⁴, where only 1 degree mis-orientation results in a clear feature of the c -axis phonons in the spectra. This remarkable effect is due to the completely insulating spectral profile for $E \parallel c$. In

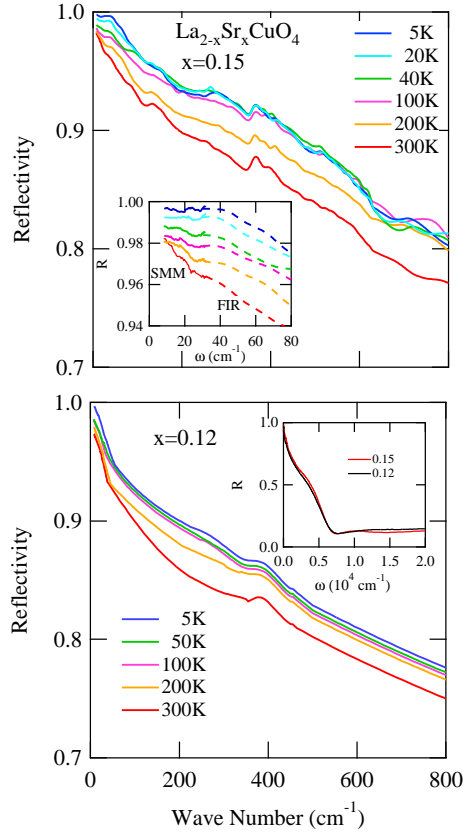


FIG. 3: Temperature dependence of in-plane reflectivity spectra of $\text{La}_{2-x}\text{Sr}_x\text{CuO}_4$ with $x=0.15$ and $x=0.12$ with $E \parallel a$ or b . The inset of the upper panel shows the spectra for $x=0.15$ in sub-millimeter (SMM) and far-infrared (FIR) regions separately. The inset of the lower panel shows the room temperature spectra in a wider range of frequency.

fact, less anisotropic materials such as well-oxygenated YBCO have never shown the c -axis component in the spectrum measured with the in-plane polarized light. Therefore, the measurement of in-plane spectrum for LSCO and probably $(\text{Nd,Ce})_2\text{CuO}_4$ requires particularly high quality samples without any multi-domain feature, high accuracy in cutting angle and careful polarization measurements. These requirements are quite severe, compared to that for other measurement techniques such as neutron scattering.

B. In-plane optical spectra

Hereafter we focus on the results of the sample for LSC#1 which we believe the purely in-plane polarized spectrum, and for comparison on the results of the $x=0.12$ sample with ac -face which was also well characterized. Figure 3 shows the in-plane reflectivity spectra for $x=0.15$ (a) and 0.12 (b) at various temperatures. Phonon peaks are almost screened by free carriers except for the small structure at $\sim 370 \text{ cm}^{-1}$ ascribed to

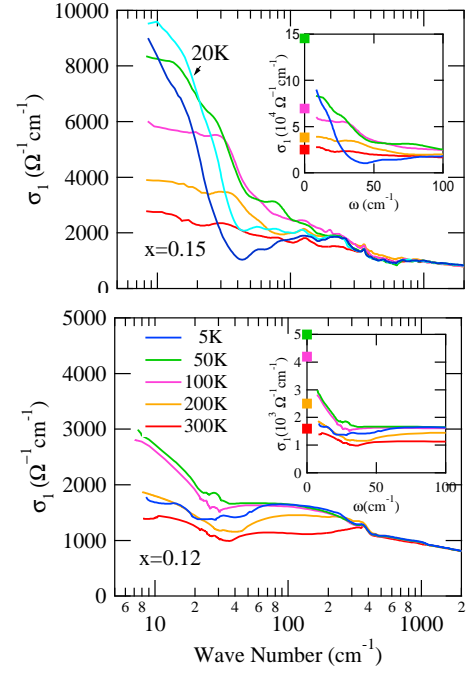


FIG. 4: Temperature dependence of in-plane conductivity spectra of $\text{La}_{2-x}\text{Sr}_x\text{CuO}_4$ with $x=0.15$ and $x=0.12$ with $E \parallel a$ or b . Inset figures show the low- ω spectra and the dc conductivity. The optical data can be smoothly extrapolated to the dc values.

the in-plane oxygen bending mode phonon. No admixture of the c -axis component is observed in both sample spectra. The FIR reflectance is smoothly connected to the sub-millimeter reflectance as shown in the inset of Fig.3(a). When the temperature is lowered below T_c , the reflectance for $x=0.15$ exhibits a rapid increase below 150 cm^{-1} and a plateau below 40 cm^{-1} , which could be originating from the condensation of low frequency spectral weight transferred to $\delta(\omega)$ at $\omega=0$. A similar feature is observed in the in-plane SC spectra of YBCO and BSCCO, but at higher frequency of $\sim 500 \text{ cm}^{-1}$, probably owing to the larger energy scale of SC gaps.

The reflectance is transformed to the complex conductivity $\sigma(\omega)$ by utilizing KK relations. Figure 4 shows the real part conductivity $\sigma_1(\omega)$ that can be smoothly extrapolated to a dc value at each temperature above T_c as shown in the inset, justifying the validity of our KK analysis. The low- ω $\sigma_1(\omega)$ for $x=0.15$ increases with reducing the temperature, forming a Drude-like peak at $\omega=0$, as is seen in Fig.4(a). When the temperature decreases below T_c , σ_1 starts to be suppressed below 250 cm^{-1} , corresponding to the SC gap opening. This SC response is, however, followed by an unusual Drude-like increase below 40 cm^{-1} even at $5\text{K} \ll T_c$. A similar Drude-like response is also seen in the low- ω upturn of the spectrum for $x=0.12$ (Fig.4(b)). The Drude-like peak width is narrower in the $x=0.12$ sample than that for $x=0.15$. A huge amount of residual conductivity at $T \ll T_c$ has also

been reported in a direct measurement of conductivity of $\text{La}_{1.84}\text{Sr}_{0.16}\text{CuO}_4$ film in the submillimeter wavelength region¹⁰. Moreover, this feature seems to be common in many HTSC such as YBCO and BSCCO⁹, which should affect the estimation of SC condensate.

To compare with the previous results of LSCO¹³, YBCO²⁵ and BSCCO²⁶, we derive an ω -dependent scattering rate $1/\tau(\omega) = (\omega_p^2/4\pi)\text{Re}[1/\sigma(\omega)]$ for $x=0.15$ as plotted in Fig.2(b). Here ω_p is obtained from the integral $\int_0^{\omega_0} \sigma_1(\omega)d\omega = \omega_p^2/8$. We take $\omega_0=10000\text{ cm}^{-1}$ so that the integral range includes the reflectance plasma edge, but is well below the charge transfer excitation energy in La_2CuO_4 ²⁷. The spectrum of $1/\tau(\omega)$ clearly shows a kink at 650 cm^{-1} at all temperatures. The kink in $1/\tau(\omega)$ is commonly observed at nearly the same frequency for all HTSC studied so far²⁶. This has been ascribed to the opening of a pseudogap above T_c and/or the coupling of carriers with a magnetic collective mode observed as a resonance peak in neutron scattering²⁸. Recently another candidate of source for this kink has been proposed by the study of angle-resolved photoemission spectroscopy (ARPES)²⁹. It was demonstrated that the kink in energy-dispersion curve of ARPES is observed at nearly the same energy in all HTSC, irrespective of presence of the magnetic resonance peak. A phonon mode is, then, proposed as the most likely origin of the kink in energy-dispersion curve of ARPES and $1/\tau(\omega)$.

The present result confirms that the kink in $1/\tau(\omega)$ exists at $700\text{--}800\text{ cm}^{-1}$ commonly in HTSC. A difference of our result for LSCO from those of YBCO and BSCCO is that the kink is observed even at room temperature in the optimally doped sample with $x=0.15$. The pseudogap temperature at this composition is expected to be $70\text{--}80\text{ K}$ from the T -dependences of in-plane resistivity and magnetization³⁰. It means that the kink structure is not related to the pseudogap opening. Another important difference is the SC-gap related suppression which is observed at $\omega \sim 100\text{ cm}^{-1}$ that is far below the kink frequency. This is in sharp contrast to the continuous development from a pseudogap to a SC gap observed in the other HTSC such as YBCO and BSCCO²⁵. The present observation indicates that the kink feature is irrelevant to a SC gap.

IV. DISCUSSIONS

A. SC condensate

The observed SC response is most naturally interpreted as the signature of formation of SC condensate associated with a SC gap opening. When a delta-function peak develops at $\omega=0$ in $\sigma_1(\omega)$ at the expense of its suppression in the low- ω region, $\sigma_2(\omega)$ behaves as proportional to ω_{ps}^2/ω . There are two ways to estimate the SC condensate ω_{ps}^2 from the optical spectrum. One is to calculate the missing area $A(= \omega_{ps}^2/8)$ in $\sigma_1(\omega)$, and the other is to estimate ω_{ps} from the slope of $\sigma_2(\omega)$ vs $1/\omega$.

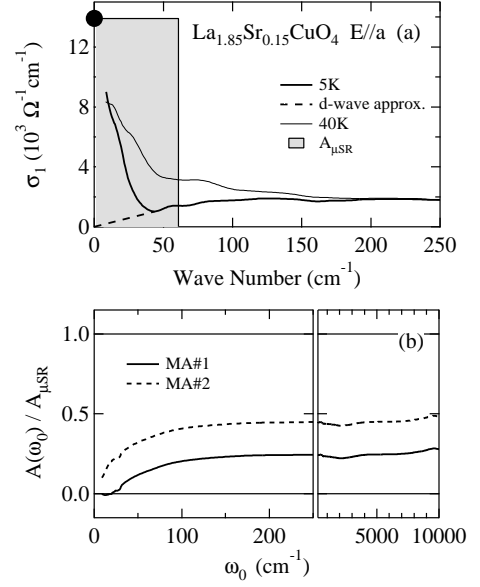


FIG. 5: (a) Optical conductivity of $\text{La}_{1.85}\text{Sr}_{0.15}\text{CuO}_4$ ($T_c=36\text{ K}$) with $E \parallel a$ or b at $T=40\text{ K}$ and 5 K . The missing area $A_{\mu\text{SR}}$ expected from $\lambda_L=280\text{ nm}$ obtained in the μSR study is shown by a hatched area. The solid circle indicates the dc conductivity at 40 K . (b) The ratio of the missing area obtained from the present optical study $A(\omega_0)$ to $A_{\mu\text{SR}}$. MA#1 represents the ratio for $A(\omega_0)$ calculated with the lower limit of integral of 8 cm^{-1} . MA#2 is for the data of $A(\omega_0)$ calculated by the dashed curve extrapolation in Fig.5(a).

In the case of HTSC, it is not a trivial issue that these two methods give an identical value of ω_{ps} , since a possibility of kinetic energy contribution has been suggested by both theory³¹ and experiment^{32,33}. We compare the two optically obtained values to check the Ferrell-Glover-Tinkham (FGT) sum rule, and also compare them with those estimated from the London penetration depths that were determined by μSR measurement.

Below, we focus on the condensate weight at the lowest temperature ($\sim 5\text{ K}$) well below T_c . The conductivity missing area for $x=0.15$ is defined by the integral

$$A(\omega_0) = \int_{0+}^{\omega_0} [\sigma_1(\omega, 40\text{ K}) - \sigma_1(\omega, 5\text{ K})] d\omega, \quad (1)$$

where we set $\omega_0 = 10000\text{ cm}^{-1}$. We first put the lower limit of the integral at 8 cm^{-1} which is the limit of our optical measurement (labeled as MA#1). In Fig.5(a), the missing area $A_{\mu\text{SR}} = 1/8(2\pi\lambda_L^{\mu\text{SR}})^2$ expected from $\lambda_L^{\mu\text{SR}} = 280\text{ nm}$ obtained by μSR study³⁴ is shown by the hatched area. It is obvious that $A_{\mu\text{SR}}$ is much larger than the missing area in the optical conductivity spectrum between 40 and 5 K . The ratio of the optical missing area $A(\omega_0)$ and the μSR value $A_{\mu\text{SR}}$ is plotted in Fig.5(b) as a function of ω_0 . $A(\omega_0)/A_{\mu\text{SR}}$ increases and then saturates to 0.25 ± 0.05 , showing no appreciable change up to 10000

cm^{-1} . The penetration depth corresponding to this value of $A(\omega_0)$ is 530 nm. Even if we eliminate the contribution of the Drude-like component at 5K and replace it by a straight line (shown by a dashed line in Fig.5(a)) which mimics a d-wave SC behavior, $A(\omega_0)/A_{\mu\text{SR}}$ amounts only to 0.5. This is plotted as a dashed curve labeled as MA#2 in Fig.5(b), giving an upper limit of the missing area (or the lower limit of $\lambda_L^{\text{FIR}}=400$ nm) in our experiment.

The anomalously small missing area is also observed for $x=0.12$. Compared to the SC condensate estimated from the μSR $\lambda_L^{\mu\text{SR}}=310$ nm, the optical conductivity missing area $A(\omega_0)$ is substantially small with the ratio $A(\omega_0=10000 \text{ cm}^{-1})/A_{\mu\text{SR}} \sim 0.1$. The optically determined penetration depth turns out to be $\sim 1\mu\text{m}$ in this case.

Strictly speaking, the missing area which is connected with the SC condensate should be calculated from the difference between the normal and the superconducting conductivity at $T=5\text{K}$. In the above estimation of $A_0(\omega_0)$, we assume that $\int \sigma_1(\omega, 40\text{K})d\omega = \int \sigma_1^n(\omega, 5\text{K})d\omega$, where $\sigma_1^n(\omega, 5\text{K})$ is the conductivity in the case that the system keeps the normal state down to $T=5\text{K}$. In a conventional metal(superconductor), this assumption holds well, because the low- T resistivity is almost constant (the residual resistivity regime). In the case of LSCO with $x=0.12$ and 0.15 , the 'normal state' resistivity realized by the application of intense magnetic fields increases weakly with lowering T below T_c ³⁵, suggestive of a 'normal' state rather similar to the conventional one. As regards the observed T -dependence of the normal-state spectrum, Fig.4 (and its inset) indicates that the frequency range where σ_1 shows an appreciable T -variation shrinks with decreasing T . For the spectrum at $T=50\text{K}$, a difference from that at $T=100\text{K}$ is seen restricted below 30 cm^{-1} . The trend suggests that the T -dependence of σ_1^n arises predominantly from the Drude term. From this, and also from the result of dc resistivity measured under intense fields, we guess that, if the normal state persists below T_c , the Drude term would not change significantly from that at T_c , and hence the difference between $\sigma_1(40\text{K})$ and $\sigma_1^n(5\text{K})$ would be small.

Another problem in estimation using eq.(1) is the possible contribution from the higher frequency spectrum. Recently the spectral weight reduction in the high energy region above 10000 cm^{-1} has been observed in BSCCO by two independent methods and the change in kinetic energy at superconducting transition has been reported^{32,33}. We have also found small T -dependence of the present spectra in the visible frequency region, which gives additional weight to $A(\omega_0=10000\text{cm}^{-1})$. However, the integral up to $\omega_0=30000 \text{ cm}^{-1}$ increases $A(\omega_0)$ only by 20% at most. The kinetic energy change, if it exists, cannot explain the small missing area in the present results.

The second method to estimate the SC condensate is to use σ_2 . In Fig.6, σ_2 is plotted as a function of $1/\omega$. It is substantially deviated from the linear-relationship, because large amount of remaining conductivity $\sigma_1(\omega)$

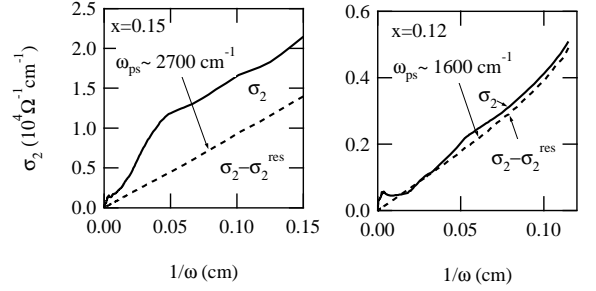


FIG. 6: Imaginary part of conductivity $\sigma_2(\omega)$ of $\text{La}_{1-x}\text{Sr}_x\text{CuO}_4$ for $x=0.12$ and 0.15 at low frequencies. $E \parallel a(b)$ and $T=5\text{K}$. σ_2^{res} is calculated from the residual $\sigma_1(\omega)$ at 5K using KK-relation. When σ_2^{res} is subtracted, σ_2 well scales with $1/\omega$, which is the signature of superconducting carrier response.

below 50 cm^{-1} strongly influences $\sigma_2(\omega)$. In order to remove the contribution of this residual conductivity, we adopt the method proposed by Dordevic *et al.*³⁶. First, we assume $\sigma_1(\omega)$ at 5K as the conductivity of unpaired carriers $\sigma_1^{\text{res}}(\omega)$ which do not condense at $\omega=0$. Next, we calculate $\sigma_2^{\text{res}}(\omega)$ corresponding to $\sigma_1^{\text{res}}(\omega)$ using a KK-relation. Then, the $\sigma_2^s(\omega)$ which should represent the "true" superfluid response is obtained as $\sigma_2^s(\omega) = \sigma_2(\omega) - \sigma_2^{\text{res}}(\omega)$.

The obtained $\sigma_2^s(\omega)$ is proportional to $1/\omega$ both for $x=0.12$ and 0.15 , indicating a SC response in this frequency range. The SC condensates giving $\lambda_L^{\text{FIR}}=990$ nm for $x=0.12$ and 590 nm for $x=0.15$ are estimated from the slopes, respectively. These are in agreement with the values ($1 \mu\text{m}$ for $x=0.12$ and 530 nm for $x=0.15$) obtained from the missing area in $\sigma_1(\omega)$. It means that this method for estimation of SC condensate is self-consistent within the optical spectra, and thus it is concluded that the FGT sum rule almost holds within an infrared frequency range. The present result does not completely exclude a possibility of small contribution from the high- ω region, namely, the kinetic energy contribution to the condensate weight, as was observed in BSCCO^{32,33}, but it is beyond the accuracy of our measurement.

The previously reported values of λ_L^{FIR} for the optimally doped LSCO range from 250 nm to 430 nm, depending on the sample and the research group but not on the T_c -value. The value estimated from the spectrum showing the c -axis component^{13,15} is not reliable, because the c -axis admixture modifies the conductivity spectrum as demonstrated in Fig.1. In fact, the estimated λ_L^{FIR} s' from their data are shorter than ours.

Another point to judge the data quality is whether the low- ω Drude-like component is observed and taken into account or not. If the remaining conductivity in the SC state is ignored, the missing area must be overestimated. The relatively larger missing area (or equivalently the shorter $\lambda_L^{\text{FIR}}=250\text{nm}$), reported in the paper by Gao¹² may partly result from this over-estimation of the miss-

TABLE I: Comparison of penetration depths estimated from FIR and μ SR measurements. (The FIR data of $\text{YBa}_2\text{Cu}_3\text{O}_y$ are for $E \parallel a$, while the μ SR data are the average within the ab -plane.)

| | $\text{La}_{2-x}\text{Sr}_x\text{CuO}_4$ | | $\text{YBa}_2\text{Cu}_3\text{O}_y$ | | $\text{Bi}_2\text{Sr}_2\text{CaCu}_2\text{O}_z$ |
|---------------------------------|--|-----------------------|-------------------------------------|-------------------------|---|
| | $x=0.15$ | $x=0.12$ | $y \approx 6.9$ | $y \approx 6.6$ | $T_c \approx 70\text{K}$ |
| $\lambda_L^{FIR}(\text{nm})$ | 400-530 | 630 ^a -990 | 160 ^b | ~ 300 ^c | 680 ^d |
| $\lambda_L^{\mu SR}(\text{nm})$ | 280 ^e | 310 ^f | 112 ^g | 170 ^g | 190 ^f |

^afrom Ref.39

^bfrom Ref.7

^cfrom Ref.42

^dfrom Ref.43

^efrom Ref.34

^ffrom Ref.17

^gfrom Ref.41

ing area, because the $5\text{K}-\sigma_1(\omega)$ was set to zero below 70 cm^{-1} . The measurement by Gorshunov *et al.*¹⁰ on the $\text{La}_{1.84}\text{Sr}_{0.16}\text{CuO}_4$ film ($T_c=39.5\text{K}$)³⁷, which covered the frequency range down to 5 cm^{-1} , clearly detected a narrow Drude-like band with the large weight $\omega_p \sim 7800\text{ cm}^{-1}$ at 5K. Subtracting the Drude-like spectral contribution by fitting, they obtained a long penetration depth $\lambda_L^{FIR}=400\text{ nm}$. A little longer penetration depth $\lambda_L^{FIR}=430\text{ nm}$ was reported by Somal *et al.*¹¹ for a single crystal. These values are in fairly good agreement with our estimate of the shorter limit of λ_L^{FIR} . Therefore, we conclude that the spectra successfully measured without contamination of the c -axis component give a similar value of λ_L (400-500 nm) that is longer than the estimate (250-310 nm) from the contaminated spectra.

The microwave (MW) conductivity measurement gives a similar large value ($=\lambda_L^{MW}=400\pm 100\text{ nm}$ for $x=0.15$) to our FIR result, although the error bar is quite large in this technique³⁸. By contrast, the μ SR penetration depth^{16,17} is clearly shorter than the FIR and microwave values. For $x=0.12$, our estimate from the FIR data is $\lambda_L^{FIR}=990\text{ nm}$, the recent FIR data for $x=0.125$ by Dumm *et al.*³⁹ shows $\lambda_L^{FIR}=630\text{ nm}$, and the microwave data for $x=0.12$ is $\lambda_L^{MW}=500\pm 200\text{ nm}$ ³⁸. Note that λ_L^{FIR} as well as T_c is very sensitive to the Sr-content x around $x=0.12$ owing to the so-called 1/8-anomaly (T_c is most suppressed when x is tuned to 0.115). Even if taking into account this situation, we can conclude that the values of λ_L^{FIR} are much longer than the μ SR estimate $\lambda_L^{\mu SR}=310\text{ nm}$.

A similar discrepancy between the FIR- and the μ SR-penetration depths is also seen in the case of YBCO and BSCCO particularly in the underdoped regime. In the optimally doped YBCO, the average value of a - and b -polarized data ($\lambda_L^{FIR}=160\text{ nm}$ for $E \parallel a$ and 117 nm for $E \parallel b$)^{6,7} is larger than the μ SR value [$\lambda_L^{\mu SR}(ab)=112\text{ nm}$]⁴¹. Comparing the conductivity spectra of optimally and under-doped YBCO^{25,40}, we find that the missing area of σ_1 in the underdoped YBCO with $T_c=56\text{-}59\text{K}$ is about 20% of that for the optimally doped one with $T_c=93\text{K}$. This suggests the penetration depth of about 300-400 nm for the underdoped YBCO. The recent esti-

mation of λ_L^{FIR} by subtracting the low- ω residual conductivity is about 250 nm for $\text{YBa}_2\text{Cu}_3\text{O}_{6.6}$ ⁴². This is much longer than the μ SR value ($\lambda_L^{\mu SR}=170\text{ nm}$)⁴¹. A longer FIR penetration depth is also reported for underdoped BSCCO with $T_c=70\text{K}$ ⁴³. Compared with the μ SR penetration depth ($\sim 190\text{ nm}$) for BSCCO with $T_c=75\text{K}$ ¹⁷, the reported value of λ_L^{FIR} ($=680\text{ nm}$) for the $T_c=70\text{K}$ sample⁴³ is extremely long. We summarize the comparison of the FIR- and μ SR-penetration depths for various HTSC in Table I. As is clearly seen in the table, the discrepancy between the FIR and μ SR data is quite robust for HTSC.

One may consider the possibility that a FIR spectrum is not correctly measured by some reason, for example, by the [110] surface geometry problem arising from the d -wave symmetric gap, as recently pointed out by Tu *et al.*⁴⁴. It is, however, unlikely because a small estimate of SC condensate was obtained by various measurements with various surface geometries.

It is also a general trend that the discrepancy becomes larger as one goes to more underdoped regime. This is suggestive of electronic inhomogeneity as a possible origin of the discrepancy. The SC order parameter may not be uniform in real space and vanish in some parts, according to the recent observation of STM on BSCCO¹. In LSCO, the stripe fluctuation may introduce electronic inhomogeneity. As we discuss below, the presence of non-superconducting area appears to be correlated with the residual conductivity in the SC state, which is responsible partly for the reduced missing area in $\sigma_1(\omega)$.

A distinct difference from the μ SR results was recognized in the impurity-substituted YBCO⁷, $\text{YBa}_2\text{Cu}_4\text{O}_8$ and many other disordered HTSC⁴⁵. Disorder, impurity or defect, decreases the FIR SC condensate ($\lambda_L^{FIR})^{-2}$ at much steeper rate than that expected from the linear $T_c-(\lambda_L^{\mu SR})^{-2}$ relationship observed by μ SR. For example, 0.4% Zn-substitution for optimally doped YBCO suppresses T_c from 93K to 85K and duplicates λ_L^{FIR} ($\sim 340\text{ nm}$ for $E \parallel a$), while $\lambda_L^{\mu SR}$ is expected to increase only 20% at most by the same Zn-substitution⁴⁶. The discrepancy between the FIR and μ SR data seems to be universal in the disordered or inhomogeneous cuprates, includ-

ing the underdoped cuprates for which STM suggests an inherent spatial modulation of the SC order parameter over a length scales of a few nm. It may follow that the FIR measurement is more sensitive to microscopic inhomogeneity than μ SR, and that the ordinary relationship between ρ_s and λ_L ($\rho_s \sim \lambda_L^{-2}$) no more holds for such microscopically inhomogeneous SC-state.

B. Low- ω residual conductivity at $T \ll T_c$

Finally we discuss the residual conductivity in the SC state. The Drude-like up-turn of conductivity towards $\omega=0$ is observed almost in all HTSC even at T well below T_c ⁹. In the present study, the low- ω Drude-like spectral weight at $T \ll T_c$ is smaller for $x=0.12$ than for $x=0.15$, the Drude-like peak width being narrower in the former. This is consistent with the general trend that the spectral weight of the residual conductivity increases with doping⁴⁷.

The low- ω conductivity remaining at $T \ll T_c$ is an indication of the presence of non-superconducting region. So far known are three types of inhomogeneous state in HTSC: (i) Presence of non-SC region within the SC area, either metallic as speculated for overdoped cuprates by FIR⁴⁸ and μ SR measurements^{49,50} or pseudogapped as observed by STM for underdoped BSCCO¹, (ii) Alternating array of anti-ferromagnetic (AF) and SC stripes⁵¹, (iii) Local suppression of the SC order around impurities such as Zn, as was directly observed by STM⁵².

The impurity-induced inhomogeneity [the case (iii)] has been investigated by many experimental techniques. In the optical spectra, Zn-substitution creates a huge residual conductivity, which dramatically depresses the missing area⁷. A similar observation was reported for the Zn-doped $\text{YBa}_2\text{Cu}_4\text{O}_8$ ⁴⁵ and in the irradiated YBCO⁵³, giving the evidence for the sensitiveness of the FIR probe to microscopic inhomogeneity.

The case (ii), the spin and charge stripe order can be considered as an "ordered" inhomogeneous state, which has been detected by neutron scattering experiment as a static order in $(\text{La,Nd,Sr})_2\text{CuO}_4$ ⁵¹, and probably as a dynamical form in LSCO⁵⁴, where the Sr-content $x=0.12$ ($\sim 1/8$) is expected to be closer to the static order. In this case, the charge stripes on which SC order might develop are separated by the AF spin domains, and would form a periodic Josephson coupled array. A weak spatial modulation of the Josephson coupling strength between the stripes, due to e.g. stripe meandering, is a possible source of the low- ω conductivity peak, as was observed in the c -axis optical response^{55,56,57}. When the

Josephson coupling strength is increased and strongly modulated spatially by decreasing an average spacing between stripes and/or by enhanced stripe fluctuation, the weight of residual conductivity would increase and be distributed over a fairly wide frequency range.

V. CONCLUSION

The in-plane polarized spectra of LSCO with $x=0.12$ and 0.15 were carefully measured. The peak at $\sim 500 \text{ cm}^{-1}$ that was observed in the previous reports and/or in some of our samples was assigned to the c -axis phonon mode (A_{2u}). Various possible sources for this admixture of c -axis spectral component were examined. Inaccurate angle of crystal cutting and/or multi-domains in the TSFZ-crystals possibly introduces some amount of the dielectric response for $E \parallel c$. Measurement on ab -face with non-polarized light or with p -polarization geometry also results in the c -axis component mixing. In any case, the problem originates from the large anisotropy in the electronic system of LSCO where only a small amount of c -axis component makes a serious effect on the in-plane spectrum, and therefore, this is the problem peculiar to a strongly anisotropic material like LSCO.

The obtained pure a/b -axis spectrum showed a clear superconducting response, the suppression of $\sigma_1(\omega)$ and $1/\omega$ -behavior of $\sigma_2(\omega)$. The estimation both from σ_1 and σ_2 give a consistent value of SC condensate, which indicates that the kinetic energy contribution is not appreciable. We find that the SC condensate is much smaller than that determined by μ SR. This discrepancy is possibly caused by microscopic inhomogeneity in the electronic state of superconducting CuO_2 -planes, probably related to the stripe fluctuation in the case of LSCO. It is guessed that FIR-measurement is a probe sensitive to disorder which suppresses the SC order parameters over a length scale of nano-meter. The inhomogeneous electronic state also seems to manifest in the spectrum as a residual Drude-like response at very low frequencies below 50 cm^{-1} in the SC state.

Acknowledgement

This work was supported by the New Energy and Industrial Technology Development Organization (NEDO) as Collaborative Research and Development of Fundamental Technologies for Superconductivity Applications, and by a COE Grant and a Grant-in-Aid For Scientific Research on Priority Area from the Ministry of Education, Japan.

* Electronic address: tajima@istec.or.jp

* Present address: National Institute for Material Science, Tsukuba, Ibaraki 305-0044, Japan.

** Permanent address: General Physics Institute, Russian

Academy of Sciences, 117942 Moscow, Russia.

*** Present address: Institute of Physics, ASCR, Na Slovance 2, 182 22 Praha, Czech Republic.

¹ S. H. Pan, J. P. O'Neal, R. L. Badzey, C. Chamon, H.

- Ding, J. R. Engelbrecht, Z. Wang, H. Eisaki, S. Uchida, A. K. Gupta, K.-W. Ng, E. W. Hudson, K. M. Lang and J. C. Davis, *Nature* **413**, 282 (2001). K. M. Lang, V. Madhavan, J. E. Hoffmann, H. Eisaki, S. Uchida and J. C. Davis, *Nature* **415**, 412 (2002).
- ² M. Norman, H. Ding, M. Randeria, J. C. Campuzano, T. Yokoya, T. Takeuchi, T. Takahashi, T. Mochiku, K. Kadowaki, P. Guptasarma and D. G. Hinks, *Nature* **392**, 157 (1998).
- ³ X. J. Zhou, P. Bogdanov, S. A. Kellar, T. Noda, H. Eisaki, S. Uchida, Z. Hussain, Z. -X. Shen, *Science* **286**, 268 (1999).
- ⁴ Z. Schlesinger, R. T. Collins, F. Holtzberg, C. Feild, S. H. Blanton, U. Welp, G. W. Crabtree, Y. Fang and J. Z. Liu, *Phys. Rev. Lett.* **65**, 801 (1990).
- ⁵ J. Schützmann, B. Gorshunov, K. F. Renk, J. Münzel, A. Zibold, H. P. Geserich, A. Erb and G. Müller-Vogt, *Phys. Rev.* **B46**, 512 (1992).
- ⁶ D. N. Basov, R. Liang, D. A. Bonn, W. N. Hardy, B. Dabrowski, M. Quijada, D. B. Tanner, J. P. Rice, D. M. Ginsberg and T. Timusk, *Phys. Rev. Lett.* **74**, 598 (1995).
- ⁷ N. L. Wang, S. Tajima, A. I. Rykov, and K. Tomimoto, *Phys. Rev.* **B57**, R11081 (1998).
- ⁸ D. B. Romero, C. D. Porter, D. B. Tanner, L. Forro, D. Mandrus, L. Mihaly, G. L. Carr and G. P. Williams, *Phys. Rev. Lett.* **68**, 1590 (1992).
- ⁹ D. B. Tanner and T. Timusk, *Physical Properties of high Temperature Superconductors III*, edited by D. M. Ginsberg (World Scientific, 1992) p.363.
- ¹⁰ B. P. Gorshunov, A. V. Pronin, A. A. Volkov, H. S. Somal, D. van der Marel, B. J. Feenstra, Y. Jaccard and J. -P. Locquet, *Physica B* **244**, 15 (1998).
- ¹¹ H. S. Somal, B. J. Feenstra, J. Schützmann, J. H. Kim, Z. H. Barber, V. H. M. Dujin, N. T. Hien, A. A. Menovsky, M. Palumbo and D. van der Marel, *Phys. Rev. Lett.* **76**, 1525 (1996).
- ¹² F. Gao, D. B. Romero, D. B. Tanner, J. Talvacchio and M. G. Forrester, *Phys. Rev.* **B47**, 1036 (1993).
- ¹³ T. Startseva, T. Timusk, A. V. Puchkov, D. N. Basov, H. A. Mook, M. Okuya, T. Kimura and K. Kishio, *Phys. Rev.* **B59**, 7184 (1998).
- ¹⁴ A. Lucarelli, S. Lupi, M. Ortolani, P. Calvani, P. Maselli, M. Capizzi, P. Giura, H. Eisaki, N. Kikugawa, T. Fujita, M. Fujita and K. Yamada, *Phys. Rev. Lett.* **90**, 037002 (2003).
- ¹⁵ M. A. Quijada, D. B. Tanner, F. C. Chou, D. C. Johnston, S. -W. Cheong, *Phys. Rev.* **B52**, 15485 (1995).
- ¹⁶ G. Aeppli, R. J. Cava, E. J. Ansaldo, J. H. Brewer, S. R. Kreitzman, G. M. Luke, D. R. Noakes and R. F. Kiefl, *Phys. Rev.* **B35**, 7129 (1987).
- ¹⁷ Y. J. Uemura et al., *Phys. Rev.* **B38**, 909 (1988). *Phys. Rev. Lett.* **62**, 2317 (1989). *ibid.* **66**, 2665 (1991).
- ¹⁸ G. Kozlov and A. Volkov, in *Applied Physics 74 Millimeter and Submillimeter Wave Spectroscopy of Solids*, ed. by G. Gruner, Springer-Verlag (Berlin, Heidelberg, 1998).
- ¹⁹ V. Fesenko et al., *Physica C* **211**, 343 (1993).
- ²⁰ J. R. Clem et al., *J. Low Temp. Phys.* **18**, 427 (1975).
- ²¹ R. T. Collins, Z. Schlesinger, G. V. Chandrashekhara and M. W. Shafer, *Phys. Rev.* **B39**, 2251 (1989).
- ²² S. Tajima, S. Uchida, D. Van der Marel and D. N. Basov, *Phys. Rev. Lett.* **91**, 129701 (2003).
- ²³ D. Van der Marel, J. H. Kim, J. Fieastra and A. Wittlin, *Phys. Rev. Lett.* **71**, 2676 (1993).
- ²⁴ A. Pimenov, A. V. Pronin, A. Loidl, A. Tsukada and M. Naito, *Phys. Rev.* **B66**, 212508 (2002).
- ²⁵ D. N. Basov, R. Liang, B. Dabrowski, D. A. Bonn, W. N. Hardy and T. Timusk, *Phys. Rev. Lett.* **77**, 4090 (1996).
- ²⁶ A. V. Puchkov, P. Fournier, D. N. Basov, T. Timusk, A. Kapitulnik and N. N. Kolesnikov, *Phys. Rev. Lett.* **77**, 3212 (1996).
- ²⁷ S. Uchida, T. Ido, H. Takagi, T. Arima, Y. Tokura and S. Tajima, *Phys. Rev.* **B43**, 7942 (1991).
- ²⁸ J. Rossat-Mignot, L. P. Regnault, C. Vettier, P. Bourges, P. Burlet, J. Bossy, Y. J. Henry and G. Lapertot, *Physica (Amsterdam)* **185-189C**, 86 (1991).
- ²⁹ A. Lanzara, P. V. Bogdanov, X. J. Zhou, S. A. Kellar, D. L. Feng, E. D. Lu, T. Yoshida, H. Eisaki, A. Fujimori, K. Kishio, J. -I. Shimoyama, T. Noda, S. Uchida, Z. Hussain and Z. X. Shen, *Nature* **412**, 510 (2001).
- ³⁰ T. Nakano, N. Momono, M. Oda and M. Ido, *J. Phys. Soc. Jpn.* **67**, 2622 (1998).
- ³¹ J. E. Hirsch and F. Marsiglio, *Phys. Rev.* **B45**, 4807 (1992). A. J. Leggett *et al.*, *Science* **274**, 1154 (1995). V. J. Emery, S. A. Kivelson and O. Zachar, *Phys. Rev.* **B56**, 6120 (1997). M. R. Norman *et al.*, *Phys. Rev.* **B61**, 14742 (2000). M. Imada and S. Onoda, *Problems in Strongly Correlated Electron Systems*, ed. by J. Bonca *et al.* (Kluwer Academic Pub., 2001) p.69.
- ³² H. J. A. Molegraaf, C. Presura, D. van der Marel, P. H. Kes and M. Li, *Science* **295**, 2241 (2002).
- ³³ A. F. Santander-Syro, R. P. S. M. Lobo, N. Bontemps, Z. Konstantinovic, Z. Li, and H. Raffy, *Europhys. Lett.* **62**, 568 (2003).
- ³⁴ R. Kadono *et al.*, unpublished.
- ³⁵ Y. Ando, G. S. Boebinger, A. Passner, T. Kimura and K. Kishio, *Phys. Rev. Lett.* **75**, 4662 (1995). G. S. Boebinger, Y. Ando, A. Passner, T. Kimura, M. Okuya, V. Shimoyama, K. Kishio, K. Tamasaku, N. Ichikawa and S. Uchida, *Phys. Rev. Lett.* **77**, 5417 (1996).
- ³⁶ S. V. Dordevic, E. J. Singley, D. N. Basov, S. Komiya, Y. Ando, E. Bucher, C. C. Homes and M. Strongin, *Phys. Rev.* **B65**, 134511 (2002).
- ³⁷ The film is subject to strain from the substrate which makes T_c higher than that for unstrained single crystal presumably due to suppression of stripe fluctuation. This would make $\omega_{ps}(\lambda_L^{FIR})$ of the film higher(shorter).
- ³⁸ T. Shibauchi, H. Kitano, K. Uchinokura, A. Maeda, T. Kimura and K. Kishio, *Phys. Rev. Lett.* **72** (1994) 2263.
- ³⁹ M. Dumm, D. N. Basov, S. Komiya, Y. Abe and Y. Ando, *Phys. Rev. Lett.* **88**, 147003 (2002).
- ⁴⁰ L. D. Rotter, Z. Schlesinger, R. T. Collins, F. Holtzberg, C. Feild, U. W. Welp, G. W. Crabtree, J. Z. Liu, Y. Fang, K. G. Vandervoort and S. Fleshler, *Phys. Rev. Lett.* **67**, 2741 (1991).
- ⁴¹ J. E. Sonier, J. H. Brewer, R. F. Kiefl, D. A. Bonn, S. R. Dunsinger, W. N. Hardy, R. Liang, W. A. MacFarlane, R. I. Miller and T. M. Riseman, D. R. Noakes, C. E. Stronach and M. F. White Jr., *Phys. Rev. Lett.* **79**, 2875 (1997).
- ⁴² C. C. Homes, S. V. Dordevic, D. A. Bonn, R. Liang and W. N. Hardy, *cond-mat/0303506*.
- ⁴³ A. F. Santander-Syro, R. P. S. M. Lobo, N. Bontemps, *Phys. Rev. Lett.* **88**, 097005 (2002).
- ⁴⁴ J. J. Tu, C. C. Homes, L. H. Greene, G. D. Gu and M. Strongin, *cond-mat/0307582*.
- ⁴⁵ D. N. Basov, B. Dabrowski and T. Timusk, *Phys. Rev. Lett.* **81**, 2132 (1998).
- ⁴⁶ B. Nachumi, A. Keren, K. Kojima, M. Larkin, G. M. Luke, J. Merrin, O. Tchernyshov, Y. J. Uemura, N. Ichikawa,

- M. Goto and S. Uchida Phys. Rev. Lett. **77**, 5421 (1996).
- ⁴⁷ J. Corson, J. Orenstein, J. N. Eckstein and I. Bozovic, Physica B **280**, 212 (2000).
- ⁴⁸ J. Schützmann, S. Tajima, S. Miyamoto and S. Tanaka, Phys. Rev. Lett. **73**, 174 (1994).
- ⁴⁹ Ch. Niedermayer, C. Bernhard, U. Binniger, H. Glückler, J. L. Tallon, E. J. Ansaldo and J. I. Budnick, Phys. Rev. Lett. **71**, 1764 (1993).
- ⁵⁰ Y. J. Uemura, A. Keren, L. P. Le, G. M. Luke, W. D. Wu, Y. Kubo, T. Manoko, Y. Shimakawa, M. Subramanian, J. L. Cobb and J. T. Markert, Nature **364**, 605 (1993).
- ⁵¹ J. Tranquada, B. Sternlieb, J. D. Axe, Y. Nakamura and S. Uchida, Nature **375**, 561 (1995).
- ⁵² S. H. Pan, E. W. Hudson, K. M. Lang, H. Eisaki, S. Uchida and J. C. Devis, Nature **403**, 746 (2003).
- ⁵³ D. N. Basov, A. V. Puchkov, R. A. Hughes, T. Strach, J. Preston, T. Timusk, D. A. Bonn, R. Liang and W. N. Hardy, Phys. Rev. B **49**, 12165 (1994).
- ⁵⁴ K. Yamada, C. H. Lee, K. Kurahashi, J. Wada, S. Wakimoto, S. Ueki, H. Kimura, Y. Endho, S. Hosoya, G. Shirane, R. J. Birgeneau, M. Greven, M. A. Kastner and Y. J. Kim, Phys. Rev. B **57**, 6165 (1998).
- ⁵⁵ D. van der Marel and A. Tsvetkov, Czech. J. Phys. **46**, 3165 (1996).
- ⁵⁶ H. Shibata and T. Yamada, Phys. Rev. Lett. **81**, 3519 (1998). T. Kakeshita, S. Uchida, K. M. Kojima, S. Adachi, S. Tajima, B. Gorshunov and M. Dressel, Phys. Rev. Lett. **86**, 4140 (2001).
- ⁵⁷ V. Zelezny, S. Tajima, D. Munzar, T. Motohashi, J. Shimoyama and K. Kishio, Phys. Rev. B **63**, 060502(R) (2001).